A time-reversal process for beam trusses subjected to impulse loads

Yves Le Guennec

Laboratoire MSSMat, ECP – F-92295 Châtenay-Malabry, France

E-mail: yves.le-guennec@ecp.fr

Éric Savin

DADS, ONERA – The French Aerospace Lab – F-92322 Châtillon cedex, France

E-mail: eric.savin@onera.fr

Didier Clouteau

Laboratoire MSSMat, ECP – F-92295 Châtenay-Malabry, France

E-mail: didier.clouteau@ecp.fr

Abstract. Spatial structures are often subjected to impulse loads which give rise to high-frequency (HF) waves. The objectives of the research outlined in this paper are twofold: (i) develop a reliable *direct* model of the transient dynamic response of built-up structures subjected to such impulse loads and (ii) use this model in a time-reversal *inverse* process in order to possibly detect the location of the shocks. The present study is more particularly focused on beam assemblies, as typically encountered in aerospace applications. At first, a transport model describing the evolution of the HF vibrational energy density in a three-dimensional beam truss is outlined, with an emphasis on the consideration of the reflection/transmission phenomena at the beam junctions. The latter contribute to spread HF waves within the entire structure, yielding a diffuse (noisy) vibrational energy field amenable to be efficiently time-reversed for the purpose of locating the source which has generated it. The time-reversal process itself is presented in a subsequent part. Its originality lies in the consideration of quadratic observables (energy densities) as the processed data. The approach is illustrated by a numerical simulation performed on a three-dimensional beam truss.

1. Introduction

Spatial structures are often subjected to impulse loads due to planned processes–like pyrotechnic shocks for solar panel unfolding on a satellite structure–or accidental events–like mechanical shocks generated by the collision with an orbital waste. Such loads propagate high-frequency (HF) waves carrying a vibrational energy that may be harmful to the structures themselves, or may disturb the functioning of the equipments attached to them [1]. Engineers have to resort to transient models in order to simulate and predict the response of mechanical systems to shock excitations. These analyses are still a challenging issue, both from a theoretical and a numerical point of view. In addition, a knowledge of the energy paths may be desirable for the design of aerospace devices or for the localization of impacts on structures. This paper focuses on an approach developed to locate impulse loads in beam trusses based on the measurement of quadratic observables (vibrational energies), and the use of a time-reversal process [2] applied to these signals.

Several classes of methods have been developed by engineers in order to predict the dynamic response of built-up structures to impact loads. Wave tracking approaches have been proposed such as the WKBJ (for Wentzel, Kramers, Brillouin, and Jeffreys) method [3] or the segment projection method [4], which are both dedicated to the HF range. Nevertheless as the number of wave reflections and transmissions at boundaries or interfaces between substructures increases, the number of rays to be tracked increases as well, leading to prohibitive numerical costs. Another class of local approach called the Vibrational Conductivity Analogy (VCA) has also been introduced [5]. VCA is based on the assumption that a diffusion-like evolution equation holds for the HF wave energy density. This is contradictory because a diffusion equation is not reversible in time, while this model arises from a wave equation which is reversible in time. One advantage of VCA is the consideration of energy densities, though. Indeed, these quantities evolve in the HF range at a typical scale comparable to the dimensions of the substructures in a built-up system [6]. This allows for numerical resolutions at a reduced numerical cost because the underlying (possibly sharp) wave fronts need not to be tracked. The model retained in this research aims to take advantage of both approaches: lower numerical costs achieved by the use of quadratic observables (energy densities) as in the VCA, while satisfying the time reversibility property of waves.

Based on a microlocal analysis of classical wave systems, it can be proved that the energy density associated with their HF solutions satisfies a Liouville-type transport equation [7]. The latter is time reversible as imposed by wave physics, and describes energy fields which are smoother than the underlying wave fields. Thus they are easier to solve numerically. Here, this so-called kinetic model is adapted to the case of three-dimensional beam trusses as done in [8]. The transport equations are solved numerically using modal or nodal discontinuous Galerkin (DG) finite elements [9] together with a strong-stability preserving (SSP) Runge-Kutta scheme [10] for time integration. DG methods have the advantage to be weakly dissipative and weakly dispersive, depending on the order of the nodal interpolation or the modal expansion. Thus they are well suited for late-time simulations. This is a much desirable feature for time-reversal experiments because time reversal performs better in cluttered media using multiply scattered waves recorded over long periods. At long times, the multiple scattering of HF waves induced by their multiple reflections and transmissions at the junctions and interfaces of a built-up structure are well described by a kinetic model in terms of the associated energy density [6]. Our objective is then to use this multiply scattered scalar field as the signal to be time reversed for the purpose of locating the source (the shock) which has generated the underlying HF waves. Thus the overall strategy of this research is the following: (i) one develops a kinetic model of HF wave propagation phenomena in terms of smoother quadratic observables, namely the associated energy densities; (ii) these data are used in time-reversal experiments in order to locate their source, after they have been multiply scattered by the beam junctions in the present case.

The paper is organized as follows. In a first section, the kinetic model for the evolution of wave energy densities is outlined, and the reflection/transmission phenomena pertaining to built-up structures are considered for the case of point junctions of several beams in a beam truss. The corresponding equations to be considered for time reversed simulations are detailed in the section 3, paying a particular attention to the treatment of the reflection/transmission phenomena in the time-reversed process. The numerical implementation and some preliminary numerical results are discussed in the section 4. The last section offers some conclusions and perspectives.

2. Kinetic model for beam trusses using Timoshenko's kinematics

The purpose of this section is to summarize the aforementioned kinetic model of HF wave propagation in a single Timoshenko beam and the reflection/transmission phenomena arising at the junctions of several beams, in order to consider complex three-dimensional beam trusses. The vibrational behavior of the beam is modeled by Timoshenko's beam kinematics [11] because it is more suitable to the HF range than the Euler-Bernoulli one. It includes the effects of rotary inertia and shear distortion. In this paper beam's material is assumed to be isotropic and its heterogeneities vary slowly in regard to the considered wavelengths. The cross-sections are assumed to be symmetric such that their geometrical and inertial centers are coincident and constitute the neutral fiber of the beam. The orthonormal axes attached to the neutral fiber will be denoted by $(\hat{\boldsymbol{e}}_1, \hat{\boldsymbol{e}}_2, \hat{\boldsymbol{e}}_3)$, $\hat{\boldsymbol{e}}_1$ being the tangent axis, and the corresponding coordinates by x, y, z. By Timoshenko's beam kinematical assumption, the displacement of a point $\boldsymbol{x}$ of the cross-section is split up into the contribution of the translation of the neutral fiber and the contribution of the rotation of the cross-section. Hence the motion of each cross-section is described by six degrees of freedom, depending on the tangent (curvilinear) coordinate x solely. In this framework, it is possible to show that the energy density $w_\alpha(x, t, k)$ of a HF wave propagating in the beam in the polarization mode α with wave vector k is the solution of the transport equation [6, 7]:

$$\partial_t w_\alpha + c_\alpha \hat{k}\, \partial_x w_\alpha = 0\,, \quad \alpha \in \mathsf{E}\,, \tag{1}$$

where $|k|$ is the wavenumber, $\hat{k} = k/|k|$ is the sign of the wavenumber, c_α is the group velocity of the mode α, and $\mathsf{E} = \{\mathrm{P}_1, \mathrm{P}_2, \mathrm{P}_3, \mathrm{T}_1, \mathrm{T}_2, \mathrm{T}_3\}$ is the set of the six possible polarizations. P_i denotes the compressional modes and T_i denotes the transverse modes for $1 \leq i \leq 3$. The group velocities are given by $c_\mathrm{P}(x) = \sqrt{E/\rho}$ for the compressional energetic waves and $c_\mathrm{T}(x) = \sqrt{\kappa\mu/\rho}$ for the transverse energetic waves, where E is the Young's modulus of the considered beam, $\kappa\mu$ is its reduced shear modulus, and ρ is its material density. One remarks that the k-dependency of the energy density w_α allows for wave crossing and superposition. The ultimate quantity to consider is the overall space-time energy density given by $\mathcal{E}(x, t) = \sum_{\alpha \in \mathsf{E}} \int_\mathbb{R} w_\alpha(x, k, t)\, dk$.

Now the propagation of the HF vibrational energy density in a single beam being described by Eqs. (1), the reflection/transmission phenomena arising at the junctions have to be considered in order to obtain the response of a full beam assembly. They contribute to couple the energy densities w_α that are partially reflected and transmitted at the junctions. These reflections and transmissions will give rise to a diffuse energy field spread over the entire truss at late times. It constitutes the noisy data used in the time-reversal process proposed in this paper. These phenomena are represented by power flow reflection/transmission coefficients for a junction of several of beams:

$$\rho^{11}_{\alpha\beta} = \frac{< \Pi^R_\alpha >}{< \Pi^I_\beta >}\,, \quad \tau^{q1}_{\alpha\beta} = \frac{< \Pi^{Tq}_\alpha >}{< \Pi^I_\beta >}\,, \tag{2}$$

where $< \Pi^R_\alpha >$ is the time average power flow of the reflected waves with the polarization $\alpha \in \mathsf{E}$, $< \Pi^{Tq}_\alpha >$ is the time average power flow of the transmitted waves with the polarization α in beam $\#q$, and $< \Pi^I_\beta >$ is the time average power flow of an incident wave with the polarization β. The time average power flows are computed from the continuity of the displacements, rotations, forces and moments at the junction [8]. It should be noted that the transport equations provided with boundary conditions corresponding to the above reflection/transmission operators and some initial conditions (the impulse loads one ultimately wish to localize) form a well-posed system.

3. Numerical time-reversal process

The aim of a time-reversal experiment is to possibly reconstruct an initial pulse from time-reversed signals. In the original setting of [2], the time-reversed signals were amplified beforehand in order to reconstruct an amplified pulse able to break up kidney stones, for example. Here the time-reversal procedure is considered for the transport equation (1) and reflection/transmission boundary conditions (2). The time-reversed energy density field $w^-_\alpha(x,k,t)$ should have the property:

$$w^-_\alpha(x,k,t) = w_\alpha(x,-k,t_{\text{end}}-t)\,, \tag{3}$$

meaning that the energy density traveling in a direction $\hat{k}$ at time t and position x in the direct configuration travels in a direction $-\hat{k}$ at time $t_{\text{end}}-t$ and position x in the reversed configuration. Now considering at first an isolated beam, the time-reversed energy density field within that beam is obtained straightforwardly: as the evolution law (1) is reversible in time, the time-reversed evolution equation is the same.

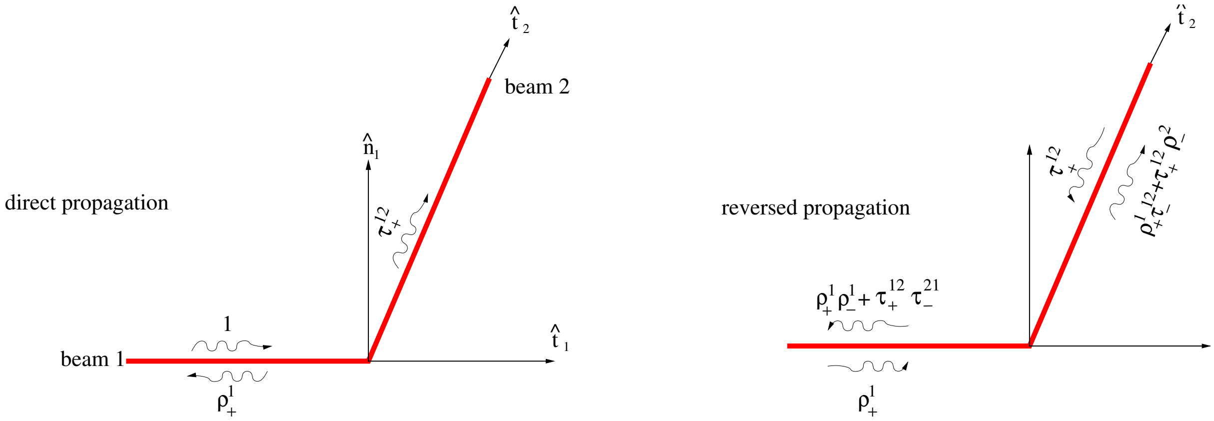

Figure 1: Energy waves in the direct propagation and their compatibility conditions for a time-reversed propagation. The wavy arrows indicate propagation directions.

The reversed-time reflection/transmission operators at the junctions have also to be derived. As shown in Figure 1, in the direct configuration, an incident energy flow normalized to 1 in the mode α generates reflected and transmitted flows of amplitudes given by the reflection/transmission coefficients given by Eqs. (2) when it impinges the junction. In the time-reversed configuration the wavenumber, and so the propagation direction, are the opposite of their direct counterparts. Thus the impinging flows are now the reflected and transmitted flows once they have been reversed in time; see Figure 1. When impinging the junction, these flows generate reflected and transmitted flows themselves, according to some reversed-time reflection/transmission operators. So the latter should be constructed such that one recovers the initial flow in mode α from the reflected/transmitted flows. These compatibility conditions yields the matrix formulation:

$$\begin{bmatrix} \boldsymbol{\rho}^1_+ & \boldsymbol{\tau}^{12}_+ \\ \boldsymbol{\tau}^{21}_+ & \boldsymbol{\rho}^2_+ \end{bmatrix} \begin{bmatrix} \boldsymbol{\rho}^1_- & \boldsymbol{\tau}^{12}_- \\ \boldsymbol{\tau}^{21}_- & \boldsymbol{\rho}^2_- \end{bmatrix} = \boldsymbol{I}\,, \tag{4}$$

where $\boldsymbol{\rho}^p_-, \boldsymbol{\tau}^{pq}_-$ are the reversed-time reflection/transmission matrices from beam $\#p$ to beam $\#q$. These operators are the unknowns of the system (4), while $\boldsymbol{\rho}^p_+$ and $\boldsymbol{\tau}^{pq}_+$ are the reflection and transmission operators for direct propagation as defined in Eq. (2). Thus it appears that the reversed-time reflection/transmission operators for the junction are simply the inverse of the direct reflection/transmission operators.

4. Numerical example

Because we lack experimental data, the signals to be time reversed are the energy density fields simulated by a direct computation up to a final time t_{end}. The transport equations are solved numerically using a discontinuous Galerkin (DG) scheme for spatial discretization [9] and an SSP Runge-Kutta scheme for time integration [10]. This numerical scheme is detailed in [8]. The goal of the simulation presented here is to test it for its use with the time-reversal process sketched in the foregoing section. Provided it is weakly dispersive and weakly dissipative, then it should be possible to retrieve an initial pulse from time-reversed simulated signals up to late times. The time-reversed simulation shall be performed using the direct energy density field computed at t_{end} as the initial pulse for that configuration, considering however an opposite direction of propagation. If the aforementioned properties of the numerical scheme are confirmed, then one argues that it can be used in a real time-reversal procedure using real data recorded from a real structure. A similar approach has been adopted in [12] for example, in order to test the time-reversal capability of a spectral finite element code solving the elastic wave equation in an unbounded, three-dimensional anisotropic random medium.

The numerical time-reversal procedure has been applied to the truss of Figure 2. The Young's moduli and beam's lengths are gathered in Tab. 1, while the Poisson's ratio is set to 0.3 for the entire truss. The direct simulation is performed up to $t_{\mathrm{end}} = 2 \times T$, where T is the time required by a transverse wave to travel across the first beam. Figure 3 shows the evolution of the energy density in the truss at selected times, and the evolution of the total energies in each beam, respectively, up to $t = 4 \times T$ after time reversal has been performed. It shows that the energy is rather uniformly spread over the entire truss at $t = t_{\mathrm{end}}$. All these plots are symmetric about t_{end}. This feature underlines the weak dissipation and weak dispersion of the numerical scheme because the evolution of the energy is symmetric for the direct and reversed simulations. Would the scheme lack these properties, it would be impossible to observe any symmetry because numerical dispersion and dissipation would have modified the signals too much to be able to retrieve the initial pulse. Here that initial pulse is indeed well retrieved.

beam $\#p$	length L_p	Young's modulus
1	5	1
2	4	0.75
3	5	1.2
4	5	1
5	2.5217	1.25
6	4	1
7	3.6988	1.25
8	5.6853	0.5
9	6.4031	1.5

Table 1: Normalized Young's moduli and beam lengths for the truss ofFigure 2.

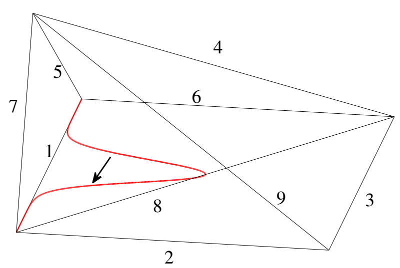

Figure 2: View of the single-bay beam truss with a Gaussian-shaped initial load in beam #1 (red line).

5. Conclusions

A kinetic model for the evolution of the vibrational energy density in Timoshenko beam assemblies has been outlined. The reflection/transmission phenomena at the beam junctions are taken into account through power flow reflection/transmission coefficients. They allow to consider complex three-dimensional beam trusses. The advantage of the model and the proposed numerical scheme is the possibility to perform numerical time-reversal experiments with quadratic observables. A numerical example has been presented showing the feasibility of this approach. Now this numerical test only constitutes the first step of a complete time-reversal

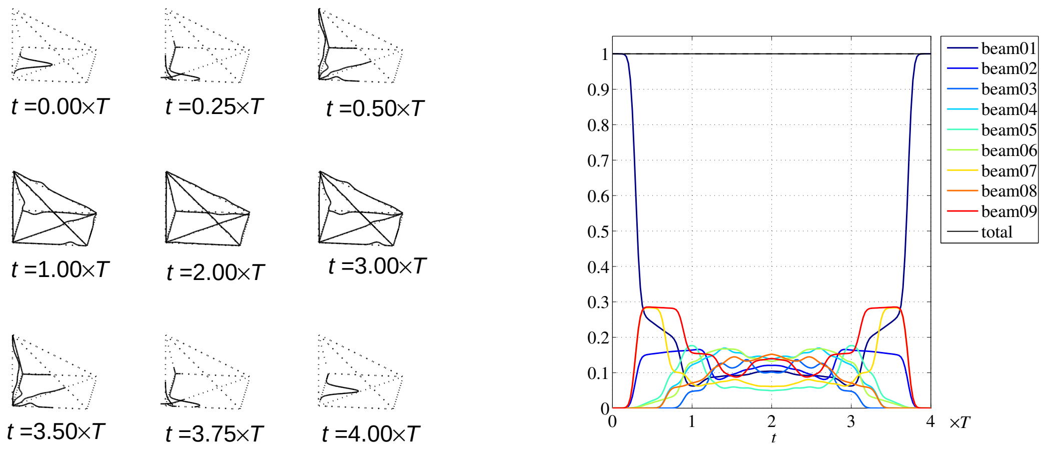

(a) Energy density evolution (b) Integrated energy density

Figure 3: (a) Direct and reversed evolution of the energy density within the truss of Figure 2 at selected times for a compressional initial pulse. Time reversal is performed at $t = 2 \times T$. (b) Evolution of the total energies $\mathcal{E}^p(t)$, $1 \leq p \leq 9$, in each beam of the truss of Figure 2.

procedure. The next step should be a stability study of the numerical scheme in order to estimate the maximum time t_{end} at which the initial pulse is still retrieved. The analysis of the effect of some noise on the numerical scheme should be performed in view of developing laboratory experiments, and time-reversal mirrors could be used subsequently. The data processed by the latter shall be the overall history of the energy density at selected points instead of the energy density recorded on the entire structure at a final time. This option has already been tested and gives satisfactory results. It will be reported in future communications.

References

[1] C. J. Moening 1986, Views of the world of pyrotechnic shock, *Shock and Vibration Bulletin*, **56**:3-28.
[2] M. Fink 1997, Time reversed acoustics, *Physics Today*, **50**:34-40.
[3] C. R. Steele 1969, Asymptotic analysis of stress waves in inhomogeneous elastic solids, *Journal of American Institute of Aeronautics and Astronautics*, **7**:896-902.
[4] B. Engquist; O. Runborg; A.-K. Tornberg 2002, High-frequency wave propagation by the segment projection method, *Journal of Computational Physics*, **178**:373-390.
[5] D. J. Nefske; S. H. Sung 1989, Power flow finite element analysis of dynamic systems: basic theory and application to beams, *ASME Journal of Vibration, Acoustics, Stress and Reliability in Design*, **111**:94-100.
[6] É. Savin 2013, High-frequency dynamics of heterogeneous slender structures, *Journal of Sound and Vibration*, **332**:2461-2487.
[7] L. Ryzhik; G. Papanicolaou; J. B. Keller 1996, Transport equations for elastic and other waves in random media, *Wave Motion*, **24**:327-370.
[8] Y. Le Guennec; É. Savin 2011, A transport model and numerical simulation of the high-frequency dynamics of three-dimensional beam trusses, *Journal of the Acoustical Society of America*, **130**:3706-3722.
[9] J. S. Hesthaven; T. Warburton 2008, *Nodal Discountinuous Galerkin Methods*, Springer.
[10] S. Gottlieb; C.-W. Shu; E. Tadmor 2001, Strong stability-preserving high-order time discretization methods, *SIAM Review*, **43**:89-112.
[11] S. P. Timoshenko 1922, On the transverse vibrations of bars of uniform cross-section, *Philosophical Magazine*, **43**:125-131.
[12] Q.-A. Ta; D. Clouteau; R. Cottereau 2010, Modeling of random anisotropic elastic media and impact on wave propagation, *European Journal of Computational Mechanics*, **19**:241-253.